www.czasopisma.pan.pl PAN POLSKA AKADEMIA NAUK www.journals.pan.pl

Arch. Metall. Mater. **65** (2020), 4, 1255-1259

DOI: 10.24425/amm.2020.133679

DA B. LEE[1,2], BONG H. KIM[1*], KWEON H. CHOI[1], SEUNG Y. YANG[1], NAM S. KIM[1], SEONG H. HA[1], YOUNG O. YOON[1], HYUN K. LIM[1], SHAE KIM[1], SOONG K. HYUN[2]

MICROSTRUCTURE AND MECHANICAL PROPERTIES OF HOT-DEFORMED AlMg4 ALLOYS WITH THE VARIATIONS OF Mn, Fe, AND Si CONTENTS

This paper aims to investigate the microstructural evolution and mechanical properties of hot-deformed AlMg4 alloys with Mn, Fe, and Si as the main impurities. For this purpose, solidification behavior and microstructural evolution during hot-rolling and heat-treatment processes are investigated by using theoretical calculations and experimental characterization. The crystallization and morphological transformation of intermetallic Al_3Fe, Al_6Mn, and Mg_2Si phases are revealed and discussed in terms of the variation in chemical composition. Following a homogenization heat-treatment, the effect of heat treatment on the intermetallic compounds is also investigated after hot-rolling. It was revealed that the Mg_2Si phase can be broken into small particles and spherodized more easily than the Al_3Fe intermetallic phase during the hot-rolling process. For the Mn containing alloys, both yield and ultimate tensile strength of the hot-rolled alloys increased from 270 to 296 MPa while elongation decreased from 17 to 13%, which can be attributed to Mn-containing intermetallic as well as dispersoid.

Keywords: Al-Mg alloy, intermetallic compounds, homogenization, hot-rolling, microstructure

1. Introduction

In the automotive industry, aluminum-magnesium alloys (5xxx series) are used for inner body panel parts and frames because of a combination of good weldability, corrosion resistance, and formability. The 5xxx series aluminum alloys, known as non-heat treatable alloys, have good mechanical properties due to the combined influence of the solid solution hardening and strain hardening mechanisms [1-4]. The material properties of the non-heat treatable Al-Mg alloys are determined by designing their alloying elements and controlling their final microstructures through manufacturing processes such as homogenization heat-treatment and hot-rolling stages.

During fabrication of the 5xxx series sheet materials, impurities originating from the raw materials, including returned scrap and equipment, are inevitable and will affect the cost and quality of the products. Fe and Si are considered the most important elemental impurities for the aluminum industry, and its alloys because they form intermetallic phases that are known to be detrimental to mechanical properties. Mn, which can present as an impurity or intentionally added, is also considered an important element to control microstructure. Depending on its amount, Mn is known to modify the morphology of various iron-containing platelet-like intermetallic compounds into less harmful shapes, like fibrous or Chinese-script morphology, during casting of aluminum alloys [4,7].

A significant amount of work has been reported on the hot-rolling and homogenization of commercial Al-Mg alloys. George Falkinger et al. [8] demonstrated the recovery behavior of AlMg4.5Mn alloys under the thermal conditions of hot-rolling. Also, Q. Zeng et al. [9] investigated the texture evolution in AA5052 alloys during hot-rolling. Tamara Radetic et al. [10] showed that the microstructure of an AA5083 alloy is governed by the distribution of alloying elements during multiple-stage homogenization treatments. However, their work was only concerned with deformation mechanisms, such as static and dynamic recrystallization, and the texture of alloys during hot processing [13-16]. Currently, to the author's knowledge, the role of Fe, Si, and Mn addition on the effects of hot-rolling and homogenization on the microstructural and mechanical properties of Al-Mg alloys have been neglected in the literature.

In the current study, the microstructural evolution of hot-deformed AlMg4 alloys, with various amounts of Fe, Si, and Mn elements, were investigated to better understand the effects

[1] ADVANCED PROCESS AND MATERIALS R&D GROUP ECO-METAL RESEARCHER CENTER, KOREA INSTITUTE OF INDUSTRIAL TECHNOLOGY, 156, GEATBEOL-RO, YEONSU-GU, INCHEON, 21999, REPUBLIC OF KOREA
[2] INHA UNIVERSITY, INCHEON, KOREA

* Corresponding author: bonghk75@kitech.re.kr

of these elements on the mechanical properties of 5xxx series aluminum alloys through conventional sheet rolling processes. For this purpose, based on the comparison of thermos-dynamical calculations of equilibrium and non-equilibrium conditions, both solidification and phase transformation were intensively discussed. Furthermore, the detailed metallurgical characterization, such as size and morphology, of intermetallic compound containing Fe, Si, and Mn were investigated through the homogenization heat-treatment and hot-rolling processes.

2. Experimental

Three alloys of AlMg4 (Alloy No.1), AlMg4Mn0.2 (Alloy No. 2), and AlMg4Fe0.3Si0.2 (Alloy No. 3) were designed for this study. The alloys were made from pure Al (99.8 wt.%) ingots, pure Mg (99.8 wt.%) ingots, and additives (tablet-shape mixture of flux and specific elements) for Fe, Si, and Mn elements by using gravity permanent mold casting. A pure Al ingot was first melted in a graphite crucible by induction heating furnace. After the complete melting of the pure Al ingot, the pure Mg and additives were added using a phosphorizer. For grain refining of the solidified microstructure, commercial Al-5Ti-B mother alloys were added to the molten metals. The molten metals were poured into a preheated permanent mold of a plate-shaped cavity (plate thickness of 20 mm with an area of 100 × 200 mm and made of steel). The chemical composition of the three alloys was analyzed by emission spectroscopy and are given in Table 1. The solidified alloys were machined into small slabs (20 mm of thickness plate with an area of 50 × 70 mm) for hot-rolling. Then, the slab samples were homogenized at 500°C for 24 h and hot-rolled from 20 to 3 mm at 500°C using a laboratory-scale rolling machine with 2-high rolls of 162 mm in diameter. Microstructural evolutions during homogenization and hot-rolling were investigated using scanning electron microscopy (SEM, QUANTA200F). The tensile properties of the hot-rolled alloys were measured by using an ultimate testing machine with a strain rate of 10^{-3} s^{-1}. Additionally, the hardness of the samples was measured using a Vickers micro-indenter with 1.4 g of applied load and 10 sec of holding time. Moreover, 10 data points were taken for each sample while the interval spacing between two spots was greater than 5 times the spot size.

TABLE 1

The chemical composition of the alloys analyzed by OES (wt%)

Alloy		Chemical composition (wt.%)							
		Si	Fe	Cu	Mn	Mg	Zn	Ti	Al
No. 1	AlMg4	0.03	0.07	0.00	0.02	4.1	0.01	0.02	bal.
No. 2	AlMg4Mn	0.03	0.07	0.00	0.18	3.9	0.01	0.02	bal.
No. 3	AlMg4FeSi	0.23	0.28	0.00	0.02	3.9	0.01	0.02	bal.

3. Results and discussion

The calculated solidification paths of the alloys are presented in Fig. 1. By using J Mat Pro software (Sente Software Ltd., U.K.), solid fractions of the constituent phases were calculated in two thermos-dynamical modes: equilibrium and non-equilibrium state. The volume fraction of each phases was plotted as a function of temperature. It appears that, despite different formation temperatures and solid fractions of each alloy, the intermetallic phases formed in the three alloys involved Al_3Fe, Al_6Mn, and Mg_2Si. In alloy No.1, various kinds of secondary intermetallic phases were expected to form with a low volume fraction of 10^{-4}. In alloy No. 2, the increasing Mn content can result in the increased formation of the Al_6Mn fraction. Furthermore, in alloy No. 3, increasing the Fe and Si contents will lead to an increase in the Al_3Fe and Mg_2Si fractions, respectively. Given that the three alloys contain sufficient Mg, the volume of Mg_2Si is, therefore, essentially determined by the amount of Si.

Fig. 2 shows the microstructures of the samples after homogenization at 500°C for 24 h. The constituent phases, indicated by the arrows and numbers in Fig. 2, were analyzed by EDS and the result are shown in Table 2. The distributions of the Mn-, Fe-, and Si-containing intermetallic compounds are observed using a scanning electron microscope. In the back-scattered electron mode, the phases bearing heavy elements (Fe and Mn) appear bright, which has light particles, most notably Mg_2Si appears dark. The majority of the bright constituent particles containing Fe is Al_3Fe (marked by yellow arrow). Moreover, as expected, the dark phases were characterized as Mg_2Si. In Fig. 2(b) of alloy No. 2, the light particles appeared as Al_6Mn while in Fig. 2(c) of alloy No.3, the light and dark particles were analyzed to be the Al_3Fe and Mg_2Si phases, respectively. The volume of the Mg_2Si phases after homogenization was found to increase, becoming larger in comparison to the as-cast state. The same constituent phases were also reported with different points of view by other researchers [4-6,17-19].

TABLE 2

Composition of intermetallic phases in Fig. 2 by SEM-EDS (at.%)

No.	Chemical compositions (at.%)						
	Al	Mg	Mn	Fe	Si	O	
Al Matrix	94.10	5.90	—	—	—	—	
1	87.66	5.22	—	7.13	—	—	Al_3Fe, Fig. 2(a)
2	67.59	19.48	—	—	12.94	—	Mg_2Si, Fig. 2(b)
3	81.84	4.33	11.58	2.25	—	—	Al_6Mn, Fig. 2(b)
4	61.82	11.47	—	—	13.28	13.43	Mg_2Si, Fig. 2(c)
5	87.23	5.59	—	7.18	—	—	Al_3Fe, Fig. 2(c)

The microstructures of the three alloys after hot-rolling at 500°C are shown in Fig. 3. In the case of hot-rolling, microstructural and morphological changes are observed for the Mg_2Si and Al_3Fe phase in the alloy. Particles were broken or merged (marked by arrow). In Fig. 3(b) and (c), comparing the

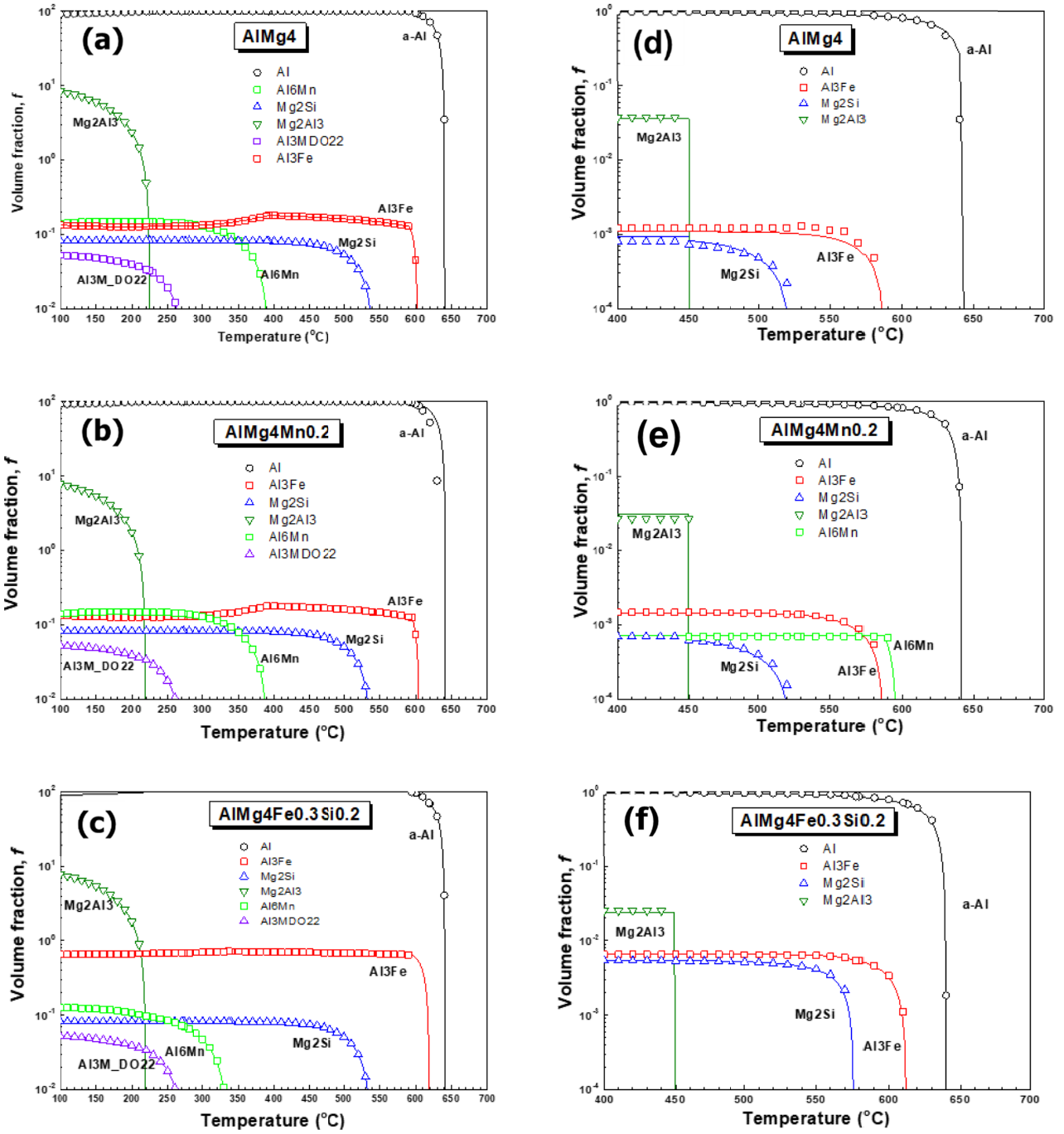

Fig. 1. Fraction solid of AlMg4, AlMg4Mn0.2 and AlMg4Fe0.3Si0.2 alloys calculated by J Mat Pro software: (a)-(c) equilibrium condition and (d)-(f) non-equilibrium condition

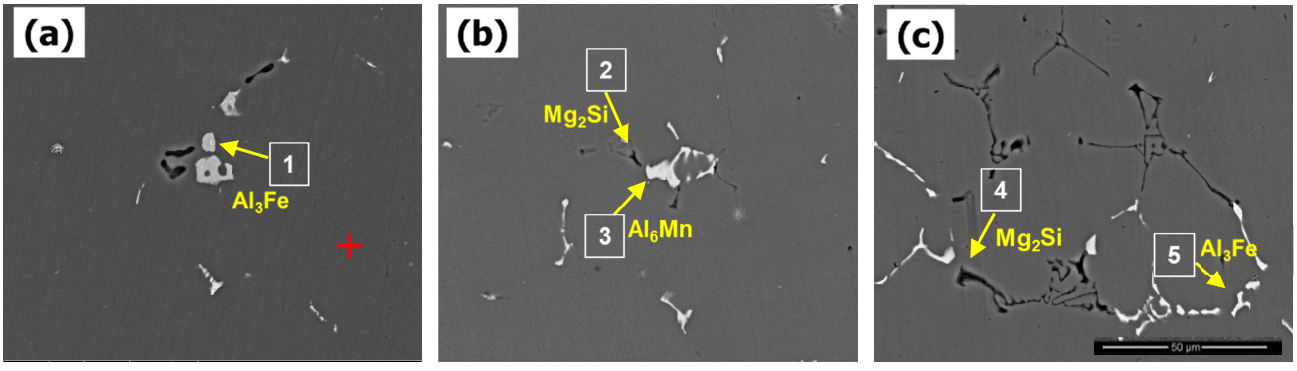

Fig. 2. Scanning electron micrographs of the samples homogenized at 500°C for 24 h: (a) AlMg4, (b) AlMg4Mn0.2 and (c) AlMg4Fe0.3Si0.2 alloy

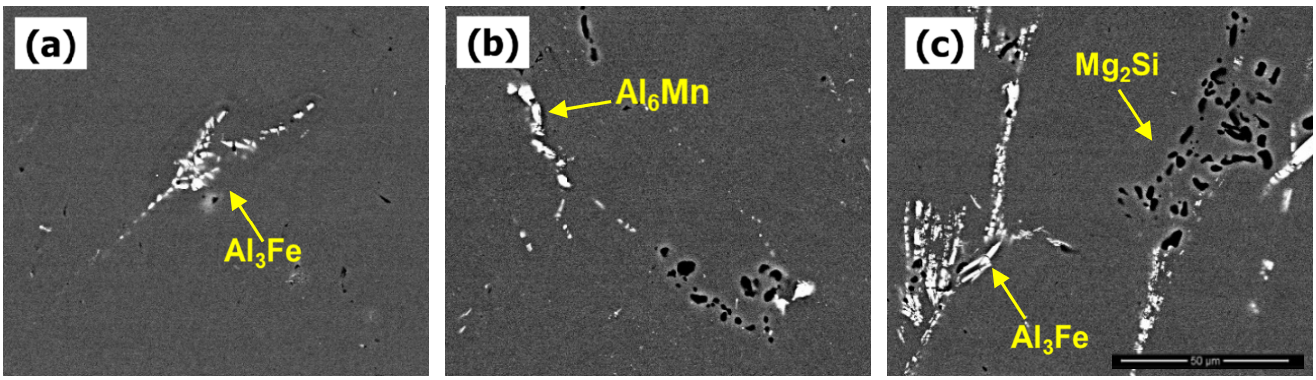

Fig. 3. Scanning electron micrographs of the hot-rolled samples showing morphology of intermetallics: (a) AlMg4, (b) AlMg4Mn0.2 and (c) AlMg4Fe0.3Si0.2 alloy

morphological differences between the intermetallic compounds, it was found that the Si-rich intermetallic compounds tend to spheroidize more than the Fe-rich phases. In addition, the presence of these particles also has an influence on the deformation, which bear upon subsequent recrystallization behaviors. Particles play an important role during recrystallization by pinning both the rearrangement of dislocations and the grain boundary migration [21].

The microstructures of hot-rolled samples analyzed at low magnification are shown in Fig. 4. The distribution of small particles, which had relatively low volume fractions as shown in Fig. 4(a), was observed in alloy No. 1. A scattered distribution of Al_6Mn was observed in alloy No. 2 while feather-like Mg_2Si and Al_3Fe phases were observed in alloy No.3. Mg atoms are well known to act as point defects within lattices and appear to obstruct the movements of dislocations. It has been reported that stationary solute atoms interact with mobile dislocations through a mechanism known as “pinning” [1,11]. On the other hand, Mn is not expected to remain in a solid solution, but rather to be involved in the formation of a dispersoid, strengthening the material by hindering the dislocation movement. For small dispersoids, the increase in strength can be predicted using the Orowan mechanism [1,12,20].

Results of the tensile test performed using the universal testing machine are shown in Table 3. It is generally known that the mechanical properties of materials highly depend on size, morphology, the distribution of intermetallics, and the matrix microstructure of the alloy [7]. The tensile properties of three samples with Mn, Fe, and Si are illustrated in Fig. 5. The yield strength (YS), ultimate tensile strength (UTS), and elongation (%) of alloy No. 1 were measured to be about 210 MPa, 270 MPa, and 17%, respectively. In alloy No.2 with Mn addition, both the YS and UTS improved to 270 MPa and 296 MPa, respectively, while a decrease in elongation from 17 to 13% was also observed. In this study, the Mn dispersoid could be expected to be an obstacle as discussed for the microstructures in Fig. 2 and 3. In alloy No. 3 with Fe and Si addition, YS and UTS slightly increased but a similar decrease in elongation to alloy No. 2 was also observed. The hardness values of the studied Al-Mg alloy samples are shown in Fig. 6. The increase in hardness from 80 to 92 in alloy No. 2 was attributed to the distribution of intermetallics as well as dispersoids. The Fe and Si-containing alloy No. 3 shows a relatively lower increase in hardness from 80 to 85.

TABLE 3

Mechanical properties of hot-rolled alloys

	Alloy	YS (MPa)	UTS (MPa)	EL (%)	Hardness (HV)
1	AlMg4	210 ±2.8	270 ±1.8	17 ±1.2	80 ±3.8
2	AlMg4Mn0.2	234 ±1.9	296 ±1.7	13 ±0.4	92 ±2.9
3	AlMg4Fe0.3Si0.2	215 ±8.8	277 ±1.5	13 ±1.1	85 ±1.7

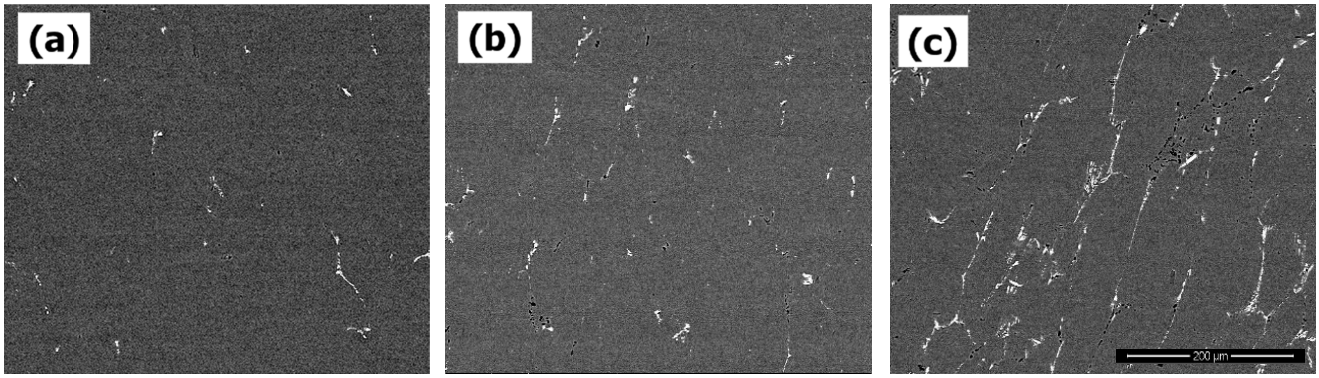

Fig. 4. Scanning electron micrographs of the hot-rolled samples showing size and distribution of intermetallics: (a) AlMg4, (b) AlMg4Mn0.2 and (c) AlMg4Fe0.3Si0.2 alloy

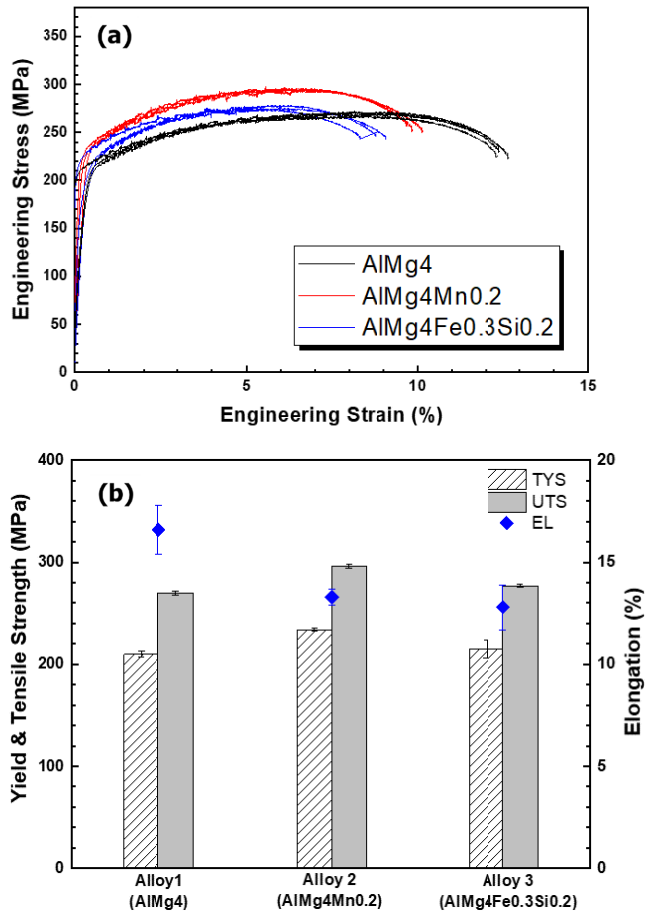

Fig. 5. Tensile properties of the hot-rolled AlMg4, AlMg4Mn0.2 and AlMg4Fe0.3Si0.2 alloy

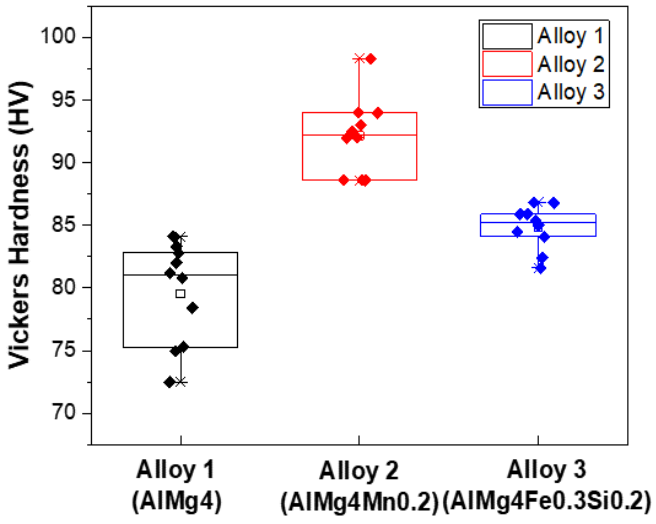

Fig. 6. Hardness properties of the hot-rolled AlMg4, AlMg4Mn0.2 and AlMg4Fe0.3Si0.2 alloy

4. Conclusions

In this article, the microstructural evolution and mechanical properties of AlMg4 alloys containing different amounts of Mn, Fe, and Si elements were investigated during homogenization and hot-rolling.

In the as-solidified state, the microstructures of three alloys revealed to contain three different but common intermetallic compounds namely Al_3Fe, Al_6Mn, and Mg_2Si, depending on their relative impurity content. The fractions of each intermetallic compound are proportional to the amount of partitioning elements. During the homogenization and hot-rolling processes, the intermetallic compounds experience morphological changes in shape, fraction, and size. The volume fraction and size of the Mg_2Si phase increase during homogenization. This phase is likely to be brittle, fractured into small pieces, and spheroidized more easily than other intermetallic phases, which could lead to a slight increase in yield and tensile strengths. On the other hand, tensile and hardness evaluation of the Mn added AlMg4 alloy revealed higher strength compared to the other alloys. It is presumably because the Mn element promotes the formation of dispersoids during the homogenization and hot-rolling processes, as well as the distribution of small particles after the hot-rolling process.

REFERENCES

[1] E.L. Huskins, Materials Science and Engineering A **527**, 1292-1298 (2010).
[2] Olaf Engler, Journal of Alloys and Compounds **689**, 998-1010 (2016).
[3] Wei Wen, Material Science and Engineering A **392**, 136-144 (2005).
[4] Olaf Engler, Journal of Alloys and Compounds **728**, 669-681 (2017).
[5] A.V. Mikhaylovskaya, Materials and Design **109**, 197-208 (2016).
[6] M. Shakiba, Materials & Engineering A **619**, 180-189(2014).
[7] Yulin Liu, Journal of Materials Science and Technology **32**, 305-312 (2016).
[8] Georg Falkinger, Procedia Engineering **207**, 31-36 (2017).
[9] Olaf Engler, Journal of Alloys and Compounds **744**, 561-573 (2018).
[10] Tamara Radetic, Materials characterization **65**, 16-27 (2012).
[11] Hao Wang, Materials Science & Engineering A **771**, 138613 (2020).
[12] Matthew R. Barnett, International Journal of Plasticity **112**, 108-122 (2019).
[13] S. Gourdet, Materials Science and Engineering A **283**, 274-288 (2000).
[14] Ke Huang, Procedia Engineering **207**, 25-30 (2017).
[15] W.C. Liu, Scripta Mterialia **52**, 1317-1321 (2005).
[16] Mohammed H. Alvi, Acta Materialia **56**, 3098-3108 (2008).
[17] Xiangzhen Zhu, Materials Science & Engineering A **732**, 240-250 (2018).
[18] Gaosong Yi, Journal of Alloys and Compounds **740**, 461-469 (2018).
[19] Gaosong Yi, Journal of Materials Science & Technology **33**, 991-1003 (2017).
[20] R. Goswami, Materials Science and Engineering A **527**, 1089-1095 (2010).
[21] J.-E. Kim, Metals and Materials International **24**, 525-531 (2018).